# Design of sEMG assembly to detect external anal sphincter activity: a proof of concept

Arsam Shiraz[1], Brian Leaker[2], Charles Alexander Mosse[3], Eskinder Solomon[4], Michael Craggs[5] and Andreas Demosthenous[1]

[1]Department of Electronic and Electrical Engineering, University College London, UK
[2]Nephro-Urology Clinical Trials (NUCT) Limited, UK
[3]Department of Medical Physics and Biomedical Engineering, University College London, UK
[4]Department of Medical Physics and Bioengineering, UCL Hospitals, UK
[5]Division of Surgery and Interventional Science, University College London, UK

E-mail: a.shiraz@ucl.ac.uk

## Abstract

*Objective:* Conditional trans-rectal stimulation of the pudendal nerve could provide a viable solution to treat hyperreflexive bladder in spinal cord injury. A set threshold of the amplitude estimate of the external anal sphincter surface electromyography (sEMG) may be used as the trigger signal. The efficacy of such a device should be tested in a large scale clinical trial. As such a probe should remain *in situ* for several hours while patients attend to their daily routine, the recording electrodes should be designed to be large enough to maintain good contact while observing design constraints. The objective of this study was to arrive at a design for intra-anal sEMG recording electrodes for the subsequent clinical trials while deriving the possible recording and processing parameters.
*Approach:* Having in mind existing solutions and based on theoretical and anatomical considerations, a set of four multi-electrode probes were designed and developed. These were tested in a healthy subject and the measured sEMG traces were recorded and appropriately processed.
*Main results:* It was shown that while comparatively large electrodes record sEMG traces that are not sufficiently correlated with the external anal sphincter contractions, smaller electrodes may not maintain a stable electrode tissue contact. It was shown that 3 mm wide and 1 cm long electrodes with 5 mm inter-electrode spacing, in agreement with Nyquist sampling, placed 1 cm from the orifice may intra-anally record a sEMG trace sufficiently correlated with external anal sphincter activity.
*Significance:* The outcome of this study can be used in any biofeedback, treatment or diagnostic application where the activity of the external anal sphincter sEMG should be detected for an extended period of time.

*Keywords:* External anal sphincter, intra-anal sEMG, sEMG electrode, surface EMG

## 1. Introduction

### *1.1. Target solution*

The activity of the external anal sphincter (EAS) may be used as a surrogate to monitor the activity of the external urethral sphincter [1]. Thus, the onset of hyperreflexive bladder contractions, which may be mirrored by external urethral sphincter contractions, may be identified by monitoring the EAS [1, 2]. This is particularly of interest in the context of conditional trans-rectal pudendal nerve stimulation, used to suppress hyperreflexive bladder contractions in spinal cord injury patients. In this case, the stimulation trigger may be recorded intra-anally in the form of a set threshold of the amplitude estimate (AE) of the EAS surface electromyography (sEMG). The sEMG sensor and the stimulator electrodes may be embedded on the same ano-rectal probe [1, 3, 4] to facilitate chronic use of this treatment in the patient group.

### *1.2. sEMG from EAS*

Anatomical studies have shown that striated EAS fibres are mainly arranged circularly around the anal canal and cross anteriorly, towards the centre of the perineum, while the fibres further away from the orifice interweave with the puborectalis muscle fibres [5]. Excluding the attempts for perianal EAS sEMG recording [6], one of the early attempts to examine the effect of electrode configuration in intra-anal EAS sEMG recording was that of Bennie *et al.* [7]. It was shown that recording as a single differential (SD) system using two longitudinal electrodes, elongated along the anal canal, separated

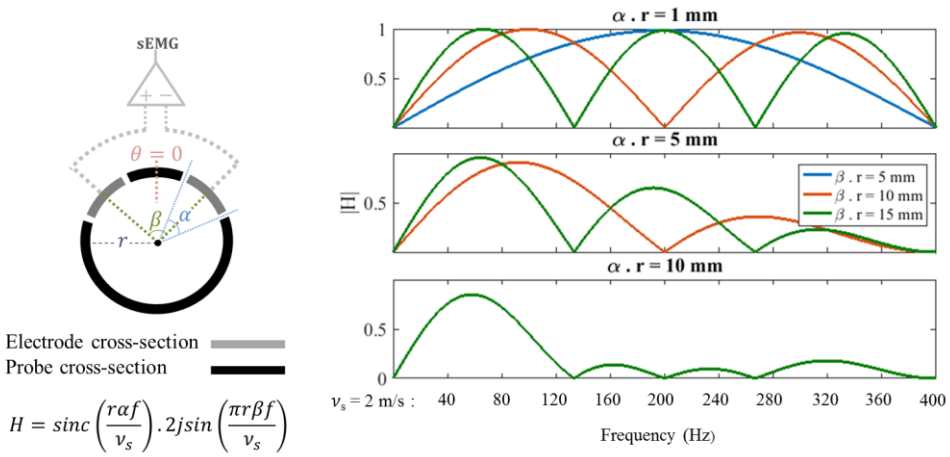


Figure 1: Cross-sectional view of differential recording using rectangular electrodes on a cylindrical probe, the transfer function of the assembly and its normalised plots for different electrode spacing and size, where $f$ is the frequency, $sinc(\theta) = \sin(\pi\theta)/\pi\theta$, $\nu_s$ is the surface velocity of the electrical potential and $j$ is $\sqrt{-1}$. For different surface velocities of the electrical potential, the temporal frequency is shifted. The frequency axis increments for $\nu_s$=2 [m.s$^{-1}$] are shown. For spatial frequency [m$^{-1}$] increments should be divided by 2.

by a distance and placed at the same distance from the orifice, considerably larger signal amplitudes are recorded compared with the signal recorded using a SD system formed of two ring electrodes placed at different distances from the orifice along the anal canal. Signals picked up by each of the ring electrodes may be more similar temporally as motor units are arranged as arcs of circles around the anal canal. Thus, SD recording using these ring electrodes may yield diminishing signals.

As action potentials travel between an innervation zone (IZ) and extinction zone (EZ) in the corresponding EAS fibres, an electrical potential distribution is induced on the surface, travelling mainly orthogonal to the anal canal [8] along the circumference of the probe. The recording points of a SD configuration placed at the same distance from the orifice, parallel with EAS fibres, sample this projection of the biopotential as it travels from one point to the other. Thus, the distance of the recording points should be informed by features such as the surface velocity of the electrical potential and its spatial frequency [9, 10]. As for the location of the points, in SD recording, it is advised to place the recording points between an IZ and EZ pair [11, 12] for reproducibility and signal strength.

As a first approximation, the electrodes may be modelled to average the electrical potential on the surface of the tissue they make contact with [13]. The width of the electrodes parallel with the fibres imposes this low-passing effect while the elongation of the electrodes along the canal records from a larger population of fibres. A trade-off between signal strength and selectivity should be sought since excessively long electrodes may record from different muscles. The electrode spacing along the circumference may also adversely affect the spatial selectivity of the detection system [11].

To quantitatively analyse the effects of some of these parameters on the recorded signal, the transfer function of the recording assembly may be found [13] as shown in figure 1. The first term of the transfer function shows the low pass filtering of the width of the electrodes in the direction of the fibres and the second term demonstrates the effect of SD recording. While further adjustments may be required for a complete representation in a cylindrical system, the model suffices for the demonstration of the points raised here. As mentioned above, the assumptions are that electrodes average the electrical potential on the surface and $\nu_s$, the surface velocity of the electrical potential, is aligned with the width of the electrodes which conform to the circumference of the cylindrical probe they are mounted on. While this model gives a first estimate of the way the recording assembly affects the recorded signal, a complete model, incorporating appropriate boundary conditions, may be developed for a more accurate representation.

The angular velocity in [rad.s$^{-1}$] of action potentials in fibres and that of the projection of the biopotential on the surface of the electrode can be assumed to be the same. However, depending on the depth of fibres and the diameter of the cylindrical probe, the velocity of the electrical potential estimated on the surface of the probe in [m.s$^{-1}$] may be considerably lower than the conduction velocity of the fibres. Experimental results suggest that the surface velocity of the electrical potential is in the region of 2 m.s$^{-1}$ [14]. The plots of transfer functions of the recording assembly versus temporal frequency increments for this surface velocity are shown in figure 1 for different electrode

size and spacing. The spatial and temporal frequencies are related by the surface velocity; thus, the increments may be converted to spatial frequency [$m^{-1}$] by dividing them by $\nu_s$=2. Possible variations in surface velocity may be accounted for in experiments by temporal oversampling. It is clear from figure 1 that larger electrode spacing shifts the first dip of the transfer function to lower frequencies and larger widths suppress higher frequencies. Therefore, knowing the maximum existent spatial frequency of the projection of biopotential on the surface, one may appropriately design a recording assembly to spatially sample the surface electrical potential while observing Nyquist rate to yield a complete and undistorted representation. The highest spatial frequency component has been reported for other muscles to be potentially as high as 90 $m^{-1}$ [10], dictating electrode spacing of about 5 mm to have the first dip of the transfer function at 200 $m^{-1}$ or higher. These apply to propagating sEMG components and not the non-propagating components due to the end-of-fibre effect [13].
Contributions involving multichannel sEMG (i.e., multiple SD recordings) have studied different anatomical features of the EAS [5, 8, 11, 14-17]. In these studies, linear arrays of rectangular electrodes were used to monitor individual motor unit action potentials to identify the positions of IZs and EZs, fibres alignment with respect to anal canal and different EAS characteristics by densely sampling the surface electrical potential. Detecting EAS activity as required in the target application, on the other hand, may be objectively performed using a SD sEMG recording and its AE [11].

### *1.3. Scope of this study*

To summarise, assuming spatial frequency properties of surface potential for intra-anal recording are similar to those reported in [10], the inter-electrode spacing should be about 5 mm and the electrode width should be as small as possible to minimise its low-pass filtering effect. The recorded sEMG signal and the quality of its AE are dependent on the status of the tissue in contact with the electrodes [18], electrode material, amplifier design and signal processing parameters as well as the anatomical features of the target muscle. As for the aforementioned target application, the device should be inserted ano-rectally to remain *in situ* for several hours in spinal cord injury patients. The associated devices (e.g., amplifier) should be portable and subsequently of moderate specifications. The primary concern in such an application is to have a stable electrode-tissue contact and avoid electrode shorting. These may not be achieved using small electrodes and short inter-electrode spacing. In addition to excessive filtering of high frequency components, larger electrodes may dictate larger inter-electrode spacing and violate basic sampling rules but may still provide usable amplitude information for this application.
In this paper, a set of multi-electrode probes with different electrode designs were developed to assess to what extent the underlying sampling rules and design considerations may be violated in favour of larger electrodes and inter-electrode spacing while the recorded signal is sufficiently correlated with the EAS activity. All the probes and different SD configurations in probes were tested in a $n$=1 study and a specific design was arrived at to be used in the subsequent clinical trials of the trans-rectal conditional neuromodulator. While a single subject study may not present a statistical case for the design, considering the way the design process was informed by the previous anatomical studies and further theoretical assessment, the proposed design is viable. Moreover, such a study in which various probes are tested intra-anally on a healthy subject may suffer from the lack of subject compliance and availability. In section 2 the methods of design, development and tests are described, followed by the results, discussions and concluding remarks in sections 3, 4 and 5, respectively.

## 2. Methods

### *2.1. Manufacturing prototypes*

Four electrode designs, whose specifications are shown in Table 1, were manufactured as shown in figure 2. The diameters of the electrode-bearing probes were 18 mm to ensure good contact while avoiding over-stretching the related structures [19]. An anchor and a 5-mm wide isthmus were devised in all designs to avoid over-insertion and facilitate orifice closure, respectively. Using probes B, C and D, the effects of electrode size, inter-electrode spacing and recording site could be tested by mounting four electrodes on them. Probe A was made to compare the results with the existing designs and devices such as Anuform (Neen Health Care, Oldham, UK) by placing the electrodes laterally. It

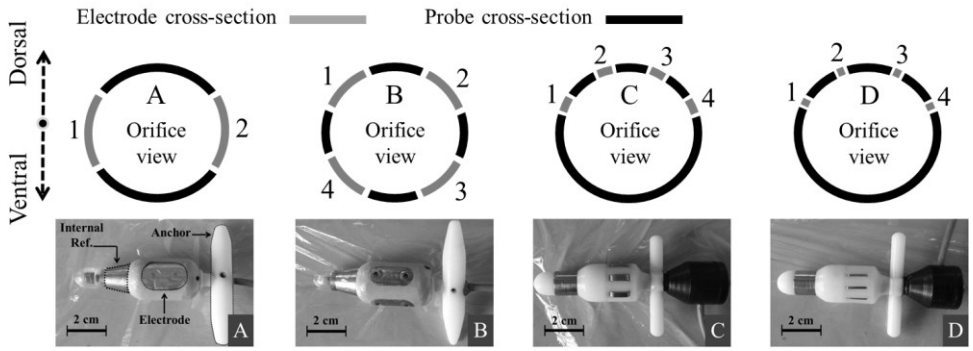


Figure 2: Diagram of the formation of the four designed and developed probes *in situ* and the actual probes.

**Table 1**: Dimensions of the electrodes on different prototypes.

| Probe | Electrode size | Electrode spacing |
|---|---|---|
| A | 15×20 mm | ~28 mm |
| B | 10×20 mm | ~15 mm |
| C | 3×10 mm | 5 mm |
| D | 1×10 mm | 5 mm |

should be noted that such a design (i.e., probe A) widely violates the appropriate spatial sampling principles and electrode placement and was only included for comparison.

Having an array of electrodes in C and D, the possibility of having at least one SD pair placed between an IZ-EZ pair [15] would be increased while the effect of a larger inter-electrode spacing could be tested. Furthermore, longer electrodes in probes A and B would test the effect of this elongation.

Medical grade stainless steel is a suitable choice for electrodes due to its mechanical properties, safe application [20] and economical availability. The body of probes A and B were made by machining solid rods of polyether ether ketone (PEEK). The anchors were made from acetal rods and the tips from acrylic rods. The electrodes were made from 316 grade stainless-steel and were screwed into recesses created in the body of the probe. The gaps at the edges of the electrodes were filled using henkel loctite hysol medical epoxy. The bodies of probes C and D were designed using FreeCAD (an open source 3D drawing package) and fabricated using 3D printing using VeroWhite material. The tip, anchor and the black cable housing compartments were made out of acetal. The electrodes were made by rolling stylets from hypodermic needles into an oval cross section and pressing them into the body like staples. This process produced rectangular electrodes with round ends. The gaps were filled using the same epoxy as before. A multi-core screened wire was used and each core was soldered to an electrode on one end and a one pole audio jack on the other.

*2.2. Protocol and apparatus*

The diagrams in figure 2 show the orientations of the probes *in situ* and the electrode numbering pattern. For each probe a set of SD configurations composed of adjacent electrodes and those with only one electrode between them was identified to be tested. This led to a total of six, five and five SD configurations in probes B, C and D, respectively (these SD configurations are referred to as *№-№* in the rest of the manuscript, where *№* is replaced by the electrode number shown in figure 2). In all cases, an external adhesive reference electrode, placed on a protruding section of the pelvis below the abdominal region of the subject, was used except one case using probe A where the effect of using an embedded reference electrode was investigated. Thus, two SD configurations were tested in probe A. A battery operated pre-amplifier with a right-leg-drive (RLD) circuit [21] was designed and implemented on a printed circuit board. The gain of the pre-amplifier was set to ×500. After a band-pass filtering stage (0.2 Hz -1062 Hz) a secondary gain stage was devised (×1-×6), yielding a total possible gain of ×3000. Using electric isolation (ISO122, a precision low-cost isolation amplifier, Texas Instruments Inc.) the subject side was isolated. An NI DAQ 6008 (National Instruments Corporation) was used to acquire signal with a 12-bit resolution at a rate of 5 Ks/s on a personal

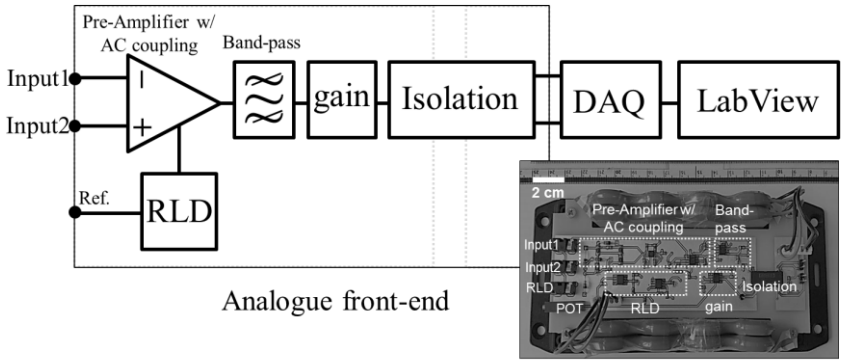


Figure 3: Block diagram of the acquisition setup and the picture of the actual custom made amplifier.

computer. Data was recorded and the signal was set to be processed in real time using LabView (National Instruments Corporation) to evaluate data during the experiments. In LabView, the raw data (digitised data after analogue front-end) and filtered data (30 Hz – 500 Hz using a 10th order digital Butterworth filter) were set to be visually inspected to better conduct the experiment and be informed of its dynamics. As discussed in section 2.4, only the raw data was then used for post-processing. Figure 3 shows the block diagram of this setting.

*2.3. Experiments*

With the approval of the local research and development review (details in Acknowledgements), the subsequent studies were performed on a male volunteer. Throughout the experiment, a clinical scientist was present as the supervisor of the experiment. Each of the devices was tested for intact electrode connectivity just prior to insertion. The probes were inserted through the anal orifice of the subject in prone position. As conductive lubricants may increase the risk of electrode shorting, a minimal amount of water based gel was applied only to the tip of the probes, and not the electrodes, for the ease of insertion as it would be necessary in this application. The same amount of lubricant was applied in all cases to ensure a fair comparison. For each configuration, the subject was prompted to contract his EAS three times separated in time, first and last times stronger than the second time. The subject was trained with the aid of the clinical scientist for appropriate contraction levels. Each contraction lasted less than 10 s and the overall recording took about 60 s for each SD configuration. The gain was set to about ×2000 as verified after the experiment by recording the value of a potentiometer which controlled the gain. The gain was set to a level such that a reasonable swing could be observed without saturation.

*2.4. Post-processing*

All the subsequent signal processing steps were performed in Matlab (MathWorks, Inc., Natick Massachusetts, US). The acquired raw signal was down-sampled to 1 Ks/s. The high-pass corner frequency was set to 30 Hz to ensure sources of artefact are sufficiently suppressed in the first stage of assessment [22-25]. The corner frequency of the low-pass filter was set to 400 Hz. A second order zero-lag Butterworth band-pass filter was implemented with the said specifications. In every case the frequency spectrum of the signal was also monitored to assess the quality of the sEMG signal using its fast Fourier transform.

Root mean square (RMS) with 1 s window in the first instance was used as the AE of the signal traces which has been shown to give an adequate and robust approximation of the AE [9, 11]. The window size was initially selected based on [1]. Traces from all the configurations were assessed based on their occurrence and intensity correlation with the EAS contractions. Further investigations were performed on the signal from probe C 1-2 configuration whose associated trace showed a comparatively higher level of correlation with the EAS contractions.

The quality of the AE is referred to as the signal to noise ratio (SNR) which is quantified as the ratio of the mean of the AE over its standard deviation [11] during sEMG activity. On a segment of the recorded signal from probe C 1-2 configuration during contraction, for high-pass corner frequencies ranging from 1 Hz to 30 Hz the SNR of the AE of the signal was calculated for different smoothing windows from 100 ms to 500 ms. Although wider smoothing windows were not tested given the

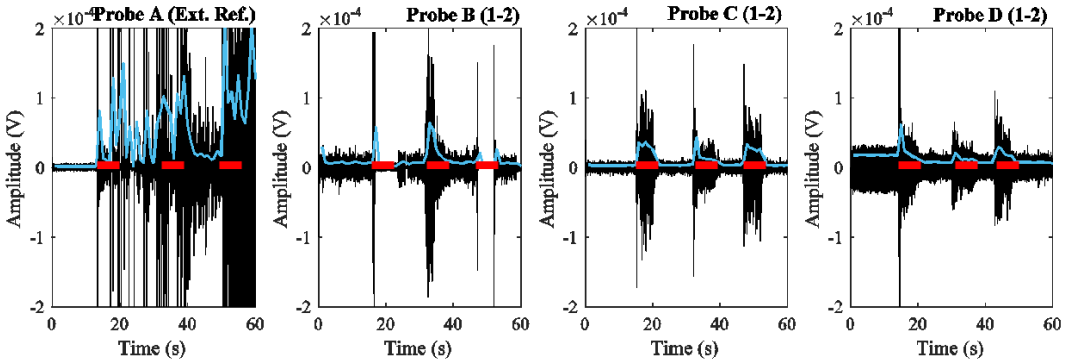


Figure 4: Sample recordings from the four probes, gain normalised and 30 Hz – 400 Hz band-passed. The red lines show when the EAS contractions were prompted while the blue traces show the RMS.

duration of contractions available, these windows are sufficiently small [1]. Finally, the effects of low-pass corner frequency and filter order on SNR were also investigated.

## 3. Results

Figure 4 shows a selected set of sEMG traces, the associated AEs and markers indicating contractions. In Probe B three configurations (1-2, 1-3 and 1-4), in probe C all the configurations and in probe D two configurations (1-2 and 2-4) showed a discernible trace of sEMG signal.

Using probe A and the external reference electrode, very little correlation with muscular activity was observed. Using the internal reference electrode, the signal was correlated with muscle activity in terms of occurrence but not intensity. A significant level of signal amplitude, presumably from other muscles, was observed for this setting in the absence of contractions. The amplitude during rest was 0.32 times that of contraction period while this should be ideally zero for a spatially selective recording system. This may be due to the reference electrode not being placed in a neutral site in this case in the context of sEMG recording.

In probe B, regardless of electrode position and spacing, moments of silence during EAS contractions were present in the sEMG traces which significantly affect the quality of the AE. This may be due to the large size of the electrodes and, consequently, their placement on either side of an IZ or EZ. In SD recording, this may result in the same spatial phases of the surface potential arriving at the site of the electrodes at the same time, resulting in zero output. The signal amplitude in rest condition was 0.22 times that of contraction period for 1-2 configuration.

In probe C, the signal was most correlated with muscular activity in which case the amplitude of the signal in the absence of contraction was only 0.07 times that of high contraction period and the sEMG amplitude of high and low contractions were distinct. Only in the case of double electrode spacing (i.e., 1-3), was extraneous activity observed which may be due to cross-talk from other muscles. Spikes were observed in the AE in the beginning of contractions which is most likely a movement artefact such as a momentary loss of contact. In probe D, presumably an unstable electrode-tissue contact using stainless steel electrodes led to the poor quality of the traces. A considerable level of mains interference was observed in the frequency spectrum of the traces of this probe which may be due to an uneven contact of the electrodes in the SD configuration which may lead to an unbalanced coupling of the interference and its differential presence at the input of the preamplifier. The mains interference was dominant during both rest and contraction periods, resulting in the amplitude of the signal during rest being as high as 0.23 times that of the high contraction period for 1-2 configuration of probe D. The mains interference was not dominant for any other of the probes, neither during rest nor contractions; hence it was assumed that the signal during rest was primarily due to cross-talk from other muscles.

Figure 5 shows the effect of variations in the SNR due to changes in the high-pass corner frequency and the RMS smoothing window length for a section of signal recorded using probe C 1-2 configuration. The inset shows the actual signal traces for different high-pass corner frequencies. It is clear that 20 Hz corner frequency with 400 ms window size yields a relatively high SNR level and

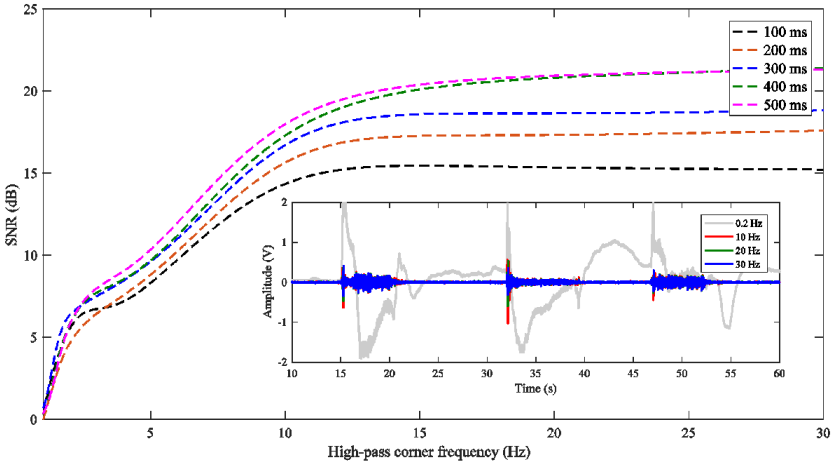


Figure 5: The SNR for different high-pass corner frequencies and RMS smoothing windows. Inset shows the traces of sEMG for different high-pass corner frequencies. This trace was recorded using probe C 1-2 configuration.

increasing the window length beyond this does not improve the SNR any further. An interesting feature of the signal is the significant level of low frequency movement artefact which is sufficiently suppressed by the shown filtering levels. The filter order beyond second and varying the low-pass corner frequency above 400 Hz did not show any improvement in the SNR.

## 4. Discussion

While it is desirable to have the surface electrodes as small as possible to minimise their low pass filtering effect, it was shown that 1 mm wide stainless electrodes do not sustain a stable contact in the target application. On the other hand, electrodes such as those on probes A and B and their inter-electrode spacing were too large, resulting in poor quality sEMG traces. This may be associated with sub-Nyquist spatial sampling of the surface potential and/or that in those cases the electrodes were placed on IZs and/or EZs. It is noted that the positions of these zones which are statistically distributed cannot be identified using a bipolar detection system. A trade-off may be reached using probe C with which it was possible to record sEMG traces that could detect EAS activity with an acceptable occurrence and intensity correlation. For the target application, a 400 ms smoothing window is sufficiently small [1] to monitor the EAS contraction as a surrogate of that of the external urethral sphincter which then may indicate hyperreflexive contractions of the bladder in spinal cord injury patients. Also, conveniently, this window is large enough to ensure a high level of the SNR.

An observation with respect to probe C was the spikes at the onset of contractions, presumably a movement artefact, which were not omitted even using relatively high high-pass corner frequencies. In a system where a relatively high threshold of the AE is set to trigger neuromodulation, this may lead to excessive stimulation which defies the purpose of having a trigger signal. Thus, a simple threshold-based trigger of the stimulus may not be sufficient and more elaborate techniques may be required for trigger strategies. The necessity of this should be ascertained in subsequent clinical trials. Given that the position of EZs and IZs may vary in different individuals [16], having an array of electrodes, it is possible to shift to different channels in case one channel is placed on these zones although signal deterioration due to recording site was not observed in this study.

While the findings here merit and assist in conducting further clinical studies, their possible limitation should be noted. In modelling the transfer function of the recording assembly, as shown in figure 1, to identify possible design avenues, a first approximation model was used. While this may be sufficient at this stage, a complete model incorporating appropriate boundary conditions may help in analysing the subsequent results. Furthermore, the assumption here was that the surface potential has similar spatial frequency characteristics to those reported for other muscles [10]. Further studies should confirm to what extend this is accurate. Moreover, depending on the outcome of the subsequent clinical studies it should be ascertained if a detailed image of EAS activity is required for the target application in which case array recording should be performed.

## 5. Conclusions

In this proof of concept study, a set of designs, informed by theoretical, anatomical and practical considerations, were tested in a healthy subject to arrive at an acceptable design for an intra-anal sEMG assembly to detect EAS activity. This design will control a conditional neuromodulator in the subsequent clinical studies on spinal cord injury patients. The findings of this study suggest that even for the detection of activity the inter-electrode spacing should be sufficiently small to observe Nyquist spatial sampling and ensure an appropriate placement. Thus, using 5 mm inter-electrode spacing for 3 mm wide electrodes it may be possible to record a sEMG signal which is sufficiently correlated with EAS activity for the target application.


## Acknowledgements

Local research and development review (UCLH) approved this experiment. Research ethics committee review is not required for research involving National Health Service (NHS) or social care staff recruited as research participants by virtue of their professional role.
www.hra.nhs.uk/resources/before-you-apply/research-requiring-nhs-rd-review-but-not-ethical-review/
This work was funded by University College London (UCL) scholarships to Arsam Shiraz and funding form Nephro-Urology Clinical Trials (NUCT) Limited.


## References


1. Knight, S.L., et al., *Conditional neuromodulation of neurogenic detrusor overactivity using transrectal stimulation in patients with spinal cord injury: A proof of principle study.* Neurourology and Urodynamics, 2017. **9999**: p. 1-9.
2. Wenzel, B.J., et al., *Detection of neurogenic detrusor contractions from the activity of the external anal sphincter in cat and human.* Neurourology and urodynamics, 2006. **25**(2): p. 140-147.
3. Shiraz, A.N., et al., *Minimizing Stimulus Current in a Wearable Pudendal Nerve Stimulator Using Computational Models.* IEEE Transactions on Neural Systems and Rehabilitation Engineering, 2016. **24**(4): p. 506-515.
4. Craggs, M., *Neuromodulation device for pelvic dysfunction, US 8644938 B2*. 2014, Nephro-Urology Clinical Trials Limited.
5. Merletti, R., et al., *Multichannel surface EMG for the non-invasive assessment of the anal sphincter muscle.* Digestion, 2004. **69**(2): p. 112-122.
6. O'Donnell, P., et al., *Surface electrodes in perineal electromyography.* Urology, 1988. **32**(4): p. 375-379.
7. Binnie, N., et al., *The importance of the orientation of the electrode plates in recording the external anal sphincter EMG by non-invasive anal plug electrodes.* International journal of colorectal disease, 1991. **6**(1): p. 5-8.
8. Cescon, C., et al., *Geometry assessment of anal sphincter muscle based on monopolar multichannel surface EMG signals.* Journal of Electromyography and Kinesiology, 2011. **21**(2): p. 394-401.
9. Afsharipour, B., K. Ullah, and R. Merletti, *Amplitude indicators and spatial aliasing in high density surface electromyography recordings.* Biomedical Signal Processing and Control, 2015. **22**: p. 170-179.
10. Soedirdjo, S., et al., *Introduction to EMG for the Study of Movement: From Bipolar to High-Density*, in *Converging Clinical and Engineering Research on Neurorehabilitation II*. 2017, Springer. p. 117-121.
11. Merletti, R. and D. Farina, *Surface electromyography: physiology, engineering and applications*. 2016: John Wiley & Sons.
12. Zaheer, F., S.H. Roy, and C.J. De Luca, *Preferred sensor sites for surface EMG signal decomposition.* Physiological measurement, 2012. **33**(2): p. 195.
13. Farina, D., et al., *A surface EMG generation model with multilayer cylindrical description of the volume conductor.* IEEE Transactions on Biomedical Engineering, 2004. **51**(3): p. 415-426.
14. Cescon, C., et al., *Characterization of the motor units of the external anal sphincter in pregnant women with multichannel surface EMG.* International urogynecology journal, 2014. **25**(8): p. 1097-1103.
15. Enck, P., et al., *Innervation zones of the external anal sphincter in healthy male and female subjects.* Digestion, 2004. **69**(2): p. 123-130.
16. Enck, P., et al., *Repeatability of innervation zone identification in the external anal sphincter muscle.* Neurourology and urodynamics, 2010. **29**(3): p. 449-457.
17. Peng, Y., et al., *Functional mapping of the pelvic floor and sphincter muscles from high-density surface EMG recordings.* International urogynecology journal, 2016: p. 1-8.
18. Merletti, R., *The electrode–skin interface and optimal detection of bioelectric signals.* Physiological measurement, 2010. **31**(10).
19. Hopkinson, B. and R. Lightwood, *Electrical treatment of incontinence.* British Journal of Surgery, 1967. **54**(9): p. 802-805.
20. Merrill, D.R., M. Bikson, and J.G. Jefferys, *Electrical stimulation of excitable tissue: design of efficacious and safe protocols*. Journal of neuroscience methods, 2005. **141**(2): p. 171-198.
21. Spinelli, E.M., R. Pallàs-Areny, and M.A. Mayosky, *AC-coupled front-end for biopotential measurements.* IEEE Transactions on Biomedical Engineering, 2003. **50**(3): p. 391-395.
22. De Luca, C.J., et al., *Filtering the surface EMG signal: Movement artifact and baseline noise contamination.* Journal of biomechanics, 2010. **43**(8): p. 1573-1579.
23. Zhou, P., B. Lock, and T.A. Kuiken, *Real time ECG artifact removal for myoelectric prosthesis control.* Physiological measurement, 2007. **28**(4): p. 397.
24. Cömert, A. and J. Hyttinen, *A motion artifact generation and assessment system for the rapid testing of surface biopotential electrodes.* Physiological measurement, 2014. **36**(1): p. 1.
25. Zhou, P. and X. Zhang, *A novel technique for muscle onset detection using surface EMG signals without removal of ECG artifacts.* Physiological measurement, 2013. **35**(1): p. 45.